PAPER

Limiting boundary correctors for periodic microstructures and inverse homogenization series

To cite this article: Fioralba Cakoni et al 2020 Inverse Problems 36 065009

View the <u>article online</u> for updates and enhancements.



IOP ebooks™

Bringing together innovative digital publishing with leading authors from the global scientific community.

Start exploring the collection-download the first chapter of every title for free.

Limiting boundary correctors for periodic microstructures and inverse homogenization series

Fioralba Cakoni¹, Shari Moskow^{2,3} and Tayler Pangburn²

- Department of Mathematics, Rutgers University, 110 Frelinghuysen Road, Piscataway, NJ 08854-8019, United States of America
- ² Department of Mathematics, Drexel University, 3141 Chestnut Street, Philadelphia, PA 19104, United States of America

E-mail: fc292@math.rutgers.edu, moskow@math.drexel.edu and tayler.anne.pangburn@drexel.edu

Received 2 January 2020, revised 8 April 2020 Accepted for publication 21 April 2020 Published 25 May 2020



Abstract

We consider the two scale asymptotic expansion for a transmission problem modeling scattering by a bounded inhomogeneity with a periodic coefficient in the lower order term of the Helmholtz equation. The squared index of refraction is assumed to be a periodic function of the fast variable, specified over the unit cell with characteristic size ϵ . Since the convergence of the boundary correctors to their limits is in general slow, we explore in detail their use in a second order approximation and show a new convergence estimate for the second order boundary corrector on a square. We show numerical examples of the higher order forward approximation in one and two dimensions. We then use the first order boundary correction as an asymptotic model for inversion and show numerical examples of inversion in the two dimensional case.

Keywords: boundary correctors, periodic inhomogeneities, inverse scattering, Helmholtz

(Some figures may appear in colour only in the online journal)

1. Introduction

The study of waves in periodic metamaterial structures is important for a broad range of applications such as medical diagnosis [17], optical super-focusing [35], energy harvesting [39], and seismic protection [18]. There is a large body of mathematics literature on waves

³Author to whom any correspondence should be addressed.

in unbounded periodic media [1, 2, 4, 5, 7, 8, 14, 15, 16, 22, 25, 27, 32, 44], however, in the above mentioned applications, the scatterer is inherently of finite extent. In recent years it was found that the boundary effects were larger than previously thought; indeed they are an order larger than periodic drift effects [12] and in some cases an order larger than bulk effects [10]. For the case of periodicity in the higher order part of the operator, explicit characterization of the boundary correctors in homogenization of periodic media has been extremely difficult, both in the case of Dirichlet [3, 6, 19, 20, 24–26, 33, 34, 41] and transmission [12, 43] problems, as well as those featuring domains with small medium perturbations [29–31], and for nonsmooth microstructures [21, 37, 38, 42]. Fortunately, it is often the case in optical scattering that the microstructure is only in the lower part of the operator (the refractive index), and in this case the most difficult aspect of the boundary corrector analysis disappears [10]. For this class of configurations, it was shown that the boundary corrector effects and limits can be both characterized explicitly and detected in the far field. We further showed that, in contrast to Dirichlet boundary value problems, the boundary effect for transmission problems emerges already at $O(\epsilon)$, where ϵ is the vanishing size of the unit cell.

While the boundary correctors limits can be characterized explicitly, convergence to these limits is often slow, and at best on the order of the characteristic cell size. In order to produce an explicitly computable approximation of the field which is higher order, one needs to augment the limiting correction with further terms. We discuss this here, in particular for the case of square scatterers for which the limits are all nontrivial (which also carries over to other convex polygons). We also show that for a square, the higher order boundary corrections converge to their limits on the order of the square root of the cell size. We validate all of these results with numerical examples. Furthermore, we explore the use of the homogenization expansion as a model for inversion and derive an exterior field asymptotic formula using the first and second order approximation to recover the periodic refractive index in the media. However, we assume we know the scatterer and the characteristic cell size and use the expansion to image the microstructure. We test this approach using the first order approximation on examples of square and circular scatterers.

The paper is organized as follows. In section 2 we discuss the problem setup and known results on the second order approximation including the boundary correction. In section 3, we consider replacing the first order correction with its limit and derive the extra terms necessary to maintain a higher order approximation. We do this explicitly for a square, and remark that the same approach works for convex polygons of rational normal. Section 4 contains a new estimate for convergence of the second order boundary correction to its limit. We show numerically the appearance and necessity of the newly derived terms in one dimension in section 5. Section 6 contains numerical examples in two dimensions, including forward approximations for a circle and square and inversion experiments for both cases. We show that if we know the homogenized scatterer (which can be obtained e.g. by qualitative inversion methods [9, 11, 13]) and the cell size, we can use the asymptotic approximation to reconstruct the microstructure.

2. Preliminaries

Let $D \subset \mathbb{R}^d$ be a bounded simply connected open set with piecewise-smooth boundary ∂D representing the support of a periodic inhomogeneity. Let $\epsilon > 0$ be the characteristic size of the periodic unit cell, which is assumed to be small both relative to the size of D and the wavelength of the incident field, and let the rescaled unit cell be defined to be $Y = [0, 1]^d$.

Assume the physical properties of an obstacle are given by a positive-definite constant matrix a and a positive scalar function $n_\epsilon:=n(x/\epsilon)\in C^\infty(D)$, related (in the context of acoustic wave propagation) to the mass density and refraction index, respectively. The slow variable is given by $x\in D$ while $y=x/\epsilon\in\mathbb{R}^d$ denotes the fast variable. The regularity restrictions on n(y) are imposed primarily for the sake of simplicity of exposition, and a more detailed investigation into minimal regularity requirements on n would be very interesting. The results here use that solutions of a constant coefficient elliptic pde with right-hand side n (see β below) have bounded gradients when restricted to the boundary, which is for example the case for a large class of piecewise smooth n. For simplicity, we also assume a and n_ϵ are real-valued, though the analysis that follows applies equally to complex coefficients, and we assume that $\inf_{|\xi|=1} \overline{\xi} \cdot a\xi = a_{\min} > 0$ and $\inf_{y\in Y} n(y) > 0$. The scattering of a time-harmonic incident field u^i (which is an entire solution of the Helmholtz equation) by the above periodic inhomogeneity can be mathematically formulated for the total field, $u=u^s+u^i$, as

$$\nabla \cdot a \nabla u + k^2 n(x/\epsilon) u = 0 \text{ in } D$$

$$\Delta u^s + k^2 u^s = 0 \text{ in } \mathbb{R}^d \backslash \overline{D}$$

$$(u^s + u^i) = u \text{ on } \partial D$$

$$\nabla (u^s + u^i) \cdot \nu = a \nabla u \cdot \nu \text{ on } \partial D$$
(1)

where $u^{\rm s}$ denotes the scattered field; the Sommerfeld radiation condition

$$\lim_{|x| \to \infty} |x|^{\frac{d-1}{2}} \left(\frac{\partial u^s}{\partial |x|} - iku^s \right) = 0 \tag{2}$$

is satisfied uniformly with respect to $\hat{x} := x/|x|$, d is the dimension of the space, and ν is the outward unit normal on ∂D .

The above scattering problem for an inhomogeneous obstacle D with periodically varying coefficients can be formulated as the transmission problem $u_{\epsilon} := u$ in D and $u_{\epsilon} := u^s$ in $\mathbb{R}^d \setminus \overline{D}$, namely

$$\nabla \cdot a \nabla u_{\epsilon} + k^{2} n(x/\epsilon) u_{\epsilon} = 0 \text{ in } D$$

$$\Delta u_{\epsilon} + k^{2} u_{\epsilon} = 0 \text{ in } \mathbb{R}^{d} \backslash \overline{D}$$

$$u_{\epsilon}^{+} - u_{\epsilon}^{-} = f \text{ on } \partial D$$

$$(\nabla u_{\epsilon} \cdot \nu)^{+} - (a \nabla u_{\epsilon} \cdot \nu)^{-} = g \text{ on } \partial D$$

$$(3)$$

where u_{ϵ} satisfies the Sommerfeld radiation condition (2) at infinity. Here $f := -u^{i}$ and $g := -\nu \cdot \nabla u^{i}$ on ∂D , and the superscripts '+' and '-' denote the respective limits on ∂D from the exterior and interior of D.

As was done in [7, 10] one can write the equation for u_{ϵ} inside of D as a first-order system

$$a\nabla u_{\epsilon} - v_{\epsilon} = 0,$$

$$\nabla \cdot v_{\epsilon} + k^{2}n(x/\epsilon)u_{\epsilon} = 0,$$
(4)

which allows one to examine the conormal jump condition more directly. We then assume an ansatz for the bulk expansions inside of D,

$$u_{\epsilon} = u_{0}(x, x/\epsilon) + \epsilon u^{(1)}(x, x/\epsilon) + \epsilon^{2} u^{(2)}(x, x/\epsilon) + \dots,$$

$$v_{\epsilon} = v_{0}(x, x/\epsilon) + \epsilon v^{(1)}(x, x/\epsilon) + \epsilon^{2} v^{(2)}(x, x/\epsilon) + \dots.$$
(5)

and we use the chain rule to write $\nabla = \nabla_x + \frac{1}{\epsilon} \nabla_y$, substitute (5) into (4), and equate the like powers of ϵ to obtain a series of equations for the interior microstructure and mean field terms. For the expansion in the exterior of D, there are no explicit microstructure terms. As was seen in [10], the exterior expansion will contain boundary corrector functions at all orders, and mean field terms beginning at second order. The boundary corrector functions are derived by matching the boundary jumps of the microstructure terms, while the mean field terms have no boundary jumps. We now summarize these results.

The homogenized solution solves the transmission problem given by

$$\nabla \cdot a \nabla u_0 + k^2 \overline{n} u_0 = 0 \text{ in } D$$

$$\Delta u_0 + k^2 u_0 = 0 \text{ in } \mathbb{R}^d \backslash \overline{D}$$

$$u_0^+ - u_0^- = f \text{ on } \partial D$$

$$(\nabla u_0 \cdot \nu)^+ - (a \nabla u_0 \cdot \nu)^- = g \text{ on } \partial D$$

$$(6)$$

with the Sommerfeld radiation condition at infinity where $\overline{n} = \int_Y n(y) \, dy$ for $Y = [0, 1] \times [0, 1]$ the period cell. One then has the second order approximation [10]

$$u_{\epsilon} = u_0 + \epsilon \theta_{\epsilon} + \epsilon^2 u^{(2)} + \epsilon^2 \theta_{\epsilon}^{(2)} + o(\epsilon^2), \tag{7}$$

where the first order boundary corrector θ_{ϵ} satisfies

$$\nabla \cdot a \nabla \theta_{\epsilon} + k^{2} n(x/\epsilon) \theta_{\epsilon} = 0 \text{ in } D$$

$$\Delta \theta_{\epsilon} + k^{2} \theta_{\epsilon} = 0 \text{ in } \mathbb{R}^{d} \backslash \overline{D}$$

$$\theta_{\epsilon}^{+} - \theta_{\epsilon}^{-} = 0 \text{ on } \partial D$$

$$(\nabla \theta_{\epsilon} \cdot \nu)^{+} - (a \nabla \theta_{\epsilon} \cdot \nu)^{-} = v^{(1)} \cdot \nu \text{ on } \partial D,$$

$$(8)$$

with the Sommerfeld radiation condition (2) at infinity. The correction $v^{(1)}$ used in the above cornormal jump is given by

$$v^{(1)} = k^2 a \nabla_{\mathbf{y}} \beta(\mathbf{y}) u_0$$

where β is the unique zero-mean *Y*-periodic solution to

$$\nabla_{\mathbf{y}} \cdot a \nabla_{\mathbf{y}} \beta(\mathbf{y}) = \overline{n} - n(\mathbf{y}).$$

The second order bulk correction, which includes the microstructure and mean field correction, is

$$u^{(2)} = k^2 \beta(y) u_0 + \hat{u}^{(2)}(x) \tag{9}$$

where the mean field drift $\hat{u}^{(2)}(x)$ is the solution to

$$\nabla \cdot a \nabla \hat{u}^{(2)} + k^2 \overline{n} \hat{u}^{(2)} = -k^4 \overline{n} \overline{\beta} u_0 \quad \text{in } D$$

$$\Delta \hat{u}^{(2)} + k^2 \hat{u}^{(2)} = 0 \quad \text{in } \mathbb{R}^d \backslash \overline{D}$$

$$(\hat{u}^{(2)})^+ - (\hat{u}^{(2)})^- = 0 \quad \text{on } \partial D$$

$$(\nabla \hat{u}^{(2)} \cdot \nu)^+ - (a \nabla \hat{u}^{(2)} \cdot \nu)^- = 0 \quad \text{on } \partial D$$

$$((10)$$

with the Sommerfeld radiation condition at infinity. The second order boundary corrector is defined to be the solution of

$$\nabla \cdot a \nabla \theta_{\epsilon}^{(2)} + k^2 n(x/\epsilon) \theta_{\epsilon}^{(2)} = 0 \quad \text{in } D$$

$$\Delta \theta_{\epsilon}^{(2)} + k^2 \theta_{\epsilon}^{(2)} = 0 \quad \text{in } \mathbb{R}^d \setminus \overline{D}$$

$$\theta_{\epsilon}^{(2)+} - \theta_{\epsilon}^{(2)-} = u^{(2)} - \hat{u}^{(2)} \quad \text{on } \partial D$$

$$(\nabla \theta_{\epsilon}^{(2)} \cdot \nu)^+ - (a \nabla \theta_{\epsilon}^{(2)} \cdot \nu)^- = (v^{(2)} - \overline{v}^{(2)}) \cdot \nu \quad \text{on } \partial D$$

$$(11)$$

with $v^{(2)}$ is given by

$$v^{(2)} = k^2 \beta(y) a \nabla u_0 + a \nabla_x \hat{u}^{(2)} - 2k^2 a (\nabla_y^2 \gamma) a \nabla u_0,$$

and the cell function γ is defined to be the Y-periodic solution to

$$\nabla_{\mathbf{v}} \cdot a \nabla_{\mathbf{v}} \gamma = \beta$$

again to be the unique Y-periodic solution with zero cell average $\int_{Y} \gamma \, dy = 0$. We note that

$$(v^{(2)} - \overline{v}^{(2)}) = k^2 \beta(y) a \nabla u_0 - 2k^2 a (\nabla_y^2 \gamma) a \nabla u_0.$$

We also characterized the general boundary correctors in section 5.3 of [10]. At each higher order ϵ^i , one will have a bulk correction $u^{(i)}$, $v^{(i)}$ which includes its mean field $\hat{u}^{(i)}$, $\overline{v}^{(i)}$. The mean field will be defined to have no transmission jumps, and the general *i*th order boundary corrector, $i = 1, 2, 3, \ldots$, will be the unique solution to

$$\nabla \cdot a \nabla \theta_{\epsilon}^{(i)} + k^{2} n(x/\epsilon) \theta_{\epsilon}^{(i)} = 0 \quad \text{in } D$$

$$\Delta \theta_{\epsilon}^{(i)} + k^{2} \theta_{\epsilon}^{(i)} = 0 \quad \text{in } \mathbb{R}^{d} \backslash \overline{D}$$

$$(\theta_{\epsilon}^{(i)})^{+} - (\theta_{\epsilon}^{(i)})^{-} = u^{(i)} - \hat{u}^{(i)} \quad \text{on } \partial D$$

$$(\nabla \theta_{\epsilon}^{(i)} \cdot \nu)^{+} - (a \nabla \theta_{\epsilon}^{(i)} \cdot \nu)^{-} = (v^{(i)} - \overline{v}^{(i)}) \cdot \nu \quad \text{on } \partial D.$$

$$(12)$$

Given that there is no oscillation in a, the asymptotic limit of these corrections is easily characterizable [10]. However, care must be taken when replacing $\theta_{\epsilon}^{(i)}$ with its limit if one needs to maintain higher order convergence. We describe in detail how this should be done for domains with flat boundary of rational normal (such as a union of period cells), and propose to use the simplified boundary corrector function defined in [10] for smooth domains with no flat parts. Furthermore, we prove a new convergence estimate for the second order boundary corrector to its limit for the case of a square. As in [10], the limit, if it exists, in general depends on how the sequence ϵ approaches zero and is slower than that of the first order correction.

3. On using limiting boundary correctors

We consider here the case of convex polygons with rational normals. In the formulation for θ_{ϵ} given in (8), the transmission data depends strongly on the choice of ϵ . If, for example D is a unit square and $\epsilon_m = 1/m$ for integer m, this boundary layer problem would see only a boundary slice of the periodic function $\nabla_y \beta$. Therefore we have different limits of the boundary layer function for different sequences of ϵ going to zero. We assume that ϵ_m is a sequence going to zero for which the boundary cutoff is fixed. That is, assume that the fractional part of $1/\epsilon_m$ is constant, i.e.

$$\delta = \frac{1}{\epsilon_m} - \lfloor \frac{1}{\epsilon_m} \rfloor \quad \text{for all } m.$$

For a sequence with fixed cutoff δ , from theorem 4.1 in [12], we have that $\theta_{\epsilon_m} \to \theta^*$ where θ^* is the solution to

$$\nabla \cdot a \nabla \theta^* + k^2 \overline{n} \theta^* = 0 \quad \text{in } D$$

$$\Delta \theta^* + k^2 \theta^* = 0 \quad \text{in } \mathbb{R}^d \backslash \overline{D}$$

$$(\theta^*)^+ - (\theta^*)^- = 0 \quad \text{on } \partial D$$

$$(\nabla \theta^* \cdot \nu)^+ - (a \nabla \theta^* \cdot \nu)^- = \overline{v^{(1)}}^{\partial} \cdot \nu \quad \text{on } \partial D$$
(13)

where $\overline{v^{(1)}}^{\partial}$ denotes the weak limit of $v^{(1)}$ on the boundary of D and is given by

$$\overline{v^{(1)}}^{\partial} = k^2 a(\nabla_{\mathbf{v}}\beta)^* u_0(x),$$

and $(\nabla_{\nu}\beta)^*$ is the weak limit of $\nabla_{\nu}\beta(x/\epsilon)$ on ∂D as $\epsilon \to 0$.

Of course one may wish to use θ^* in the approximation (7) for u_ϵ since it is much easier to compute. In this case, care must be taken as the convergence of θ_ϵ to θ^* is $O(\epsilon)$ for this case described above (and slower than that for general domains). So, while second order convergence is maintained, to obtain a higher order approximation this is insufficient. Recall that θ_ϵ and θ^* differ in both the oscillating coefficient and boundary data. Consider an auxilliary function ψ_ϵ which has the oscillating coefficient but the limiting boundary data, that is, we let ψ_ϵ satisfy

$$\nabla \cdot a \nabla \psi_{\epsilon} + k^{2} n(x/\epsilon) \psi_{\epsilon} = 0 \quad \text{in } D$$

$$\Delta \psi_{\epsilon} + k^{2} \psi_{\epsilon} = 0 \quad \text{in } \mathbb{R}^{d} \backslash \overline{D}$$

$$(\psi_{\epsilon})^{+} - (\psi_{\epsilon})^{-} = 0 \quad \text{on } \partial D$$

$$(\nabla \psi_{\epsilon} \cdot \nu)^{+} - (a \nabla \psi_{\epsilon} \cdot \nu)^{-} = \overline{v^{(1)}}^{\partial} \cdot \nu \quad \text{on } \partial D.$$

$$(14)$$

We then write

$$\epsilon \theta_{\epsilon} = \epsilon (\theta_{\epsilon} - \psi_{\epsilon}) + \epsilon (\psi_{\epsilon} - \theta^{*}) + \epsilon \theta^{*} \tag{15}$$

and note that $\theta_\epsilon - \psi_\epsilon$ satisfies the oscillatory equation and has transmission data

$$(\theta_{\epsilon} - \psi_{\epsilon})^{+} - (\theta_{\epsilon} - \psi_{\epsilon})^{-} = 0$$
$$(\nabla(\theta_{\epsilon} - \psi_{\epsilon}) \cdot \nu)^{+} - (a\nabla(\theta_{\epsilon} - \psi_{\epsilon}) \cdot \nu)^{-} = \left(v^{(1)} - \overline{v^{(1)}}^{\partial}\right) \cdot \nu.$$

We know from our analysis in [12] that if the conormal jump is divided by ϵ the bounded limit is maintained, and hence we can move this portion of the error into the *second order boundary correction*. We therefore define an adjusted second order boundary corrector $\hat{\theta}_{\epsilon}^{(2)}$ to be the solution of

$$\nabla \cdot a \nabla \hat{\theta}_{\epsilon}^{(2)} + k^{2} n(x/\epsilon) \hat{\theta}_{\epsilon}^{(2)} = 0 \quad \text{in } D$$

$$\Delta \hat{\theta}_{\epsilon}^{(2)} + k^{2} \hat{\theta}_{\epsilon}^{(2)} = 0 \quad \text{in } \mathbb{R}^{d} \setminus \overline{D}$$

$$\left(\hat{\theta}_{\epsilon}^{(2)}\right)^{+} - \left(\hat{\theta}_{\epsilon}^{(2)}\right)^{-} = u^{(2)} - \hat{u}^{(2)} = k^{2} \beta(y) u_{0}(x) \quad \text{on } \partial D$$

$$(\nabla \hat{\theta}_{\epsilon}^{(2)} \cdot \nu)^{+} - (a \nabla \hat{\theta}_{\epsilon}^{(2)} \cdot \nu)^{-} = \left(\frac{v^{(1)} - \overline{v^{(1)}} \partial}{\epsilon} + v^{(2)} - \overline{v}^{(2)}\right) \cdot \nu \quad \text{on } \partial D$$

$$(16)$$

which we know is bounded in L^2 [12]. This will take care of the first term in the right-hand side of (15). For the term $\psi_{\epsilon} - \theta^*$ we note that this corresponds to the error in a standard homogenization problem, and the largest part is taken by its boundary correction. Hence we introduce the first order limiting boundary corrector to ψ_{ϵ} , which we will call θ^{**} , to be the solution to

$$\nabla \cdot a \nabla \theta^{**} + k^2 \overline{n} \theta^{**} = 0 \quad \text{in } D$$

$$\Delta \theta^{**} + k^2 \theta^{**} = 0 \quad \text{in } \mathbb{R}^d \backslash \overline{D}$$

$$\theta^{**+} - \theta^{**-} = 0 \quad \text{on } \partial D$$

$$(\nabla \theta^{**} \cdot \nu)^+ - (a \nabla \theta^{**} \cdot \nu)^- = k^2 (a \nabla_y \beta)^* \theta^*(x) \quad \text{on } \partial D.$$

$$(17)$$

Thus, for the case of convex polygons with rational normals, our second order approximation with the first order limiting boundary corrector is

$$u_{\epsilon} = u_0 + \epsilon \theta^* + \epsilon^2 \theta^{**} + \epsilon^2 u^{(2)} + \epsilon^2 \hat{\theta}_{\epsilon}^{(2)} + o(\epsilon^2). \tag{18}$$

In this case, the limit of $\hat{\theta}_{\epsilon}^{(2)}$ as $\epsilon \to 0$ is the same as the limit of $\theta_{\epsilon}^{(2)}$, which we denote as $\theta^{(2)^*}$, and is the solution to

$$\nabla \cdot a \nabla \theta^{(2)*} + k^2 \overline{n} \theta^{(2)*} = 0 \quad \text{in } D$$

$$\Delta \theta^{(2)*} + k^2 \theta^{(2)*} = 0 \quad \text{in } \mathbb{R}^d \backslash \overline{D}$$

$$(\theta^{(2)*})^+ - (\theta^{(2)*})^- = k^2 \beta^* u_0(x) \quad \text{on } \partial D$$

$$(\nabla \theta^{(2)*} \cdot \nu)^+ - (a \nabla \theta^{(2)*} \cdot \nu)^- = (\overline{v^{(2)}} \partial \cdot \nu) \quad \text{on } \partial D$$

$$(19)$$

where β^* is the weak limit on the boundary as proven in [10]. When a doubly periodic function on \mathbb{R}^2 is restricted to a line of rational slope, its restriction is *one dimensionally periodic on that line*. Its weak limit as the period goes to zero will be the one dimensional cell average corresponding to that line. Therefore, when D is a polygon of rational sides, β^* will be constant on each flat portion of ∂D , equal to its restricted one dimensional cell average. In summary, for the case of polygons with rational normals, the second order approximation to u_{ϵ} with limiting boundary correctors at first and second order is

$$u_{\epsilon} = u_0 + \epsilon \theta^* + \epsilon^2 \theta^{**} + \epsilon^2 u^{(2)} + \epsilon^2 \theta^{(2)*} + o(\epsilon^2). \tag{20}$$

Remark 3.1. From [10], in the case where D is a domain whose boundary has no flat parts of rational normal, the limit $(\nabla_y \beta)^*$ will be its Y cell average and therefore zero as it is a gradient of a Y-periodic function. Thus θ^* and θ^{**} are identically zero, and the above approximation is essentially a reshuffling of the first order correction into the second one. Recall that the order of convergence of θ_ϵ to $\theta^* \equiv 0$ may be slow, and therefore we introduce the intermediary boundary correction $\tilde{\theta}_\epsilon$ which satisfies

$$\nabla \cdot a \nabla \tilde{\theta}_{\epsilon} + k^{2} \overline{n} \tilde{\theta}_{\epsilon} = 0 \quad \text{in } D$$

$$\Delta \tilde{\theta}_{\epsilon} + k^{2} \tilde{\theta}_{\epsilon} = 0 \quad \text{in } \mathbb{R}^{d} \backslash \overline{D}$$

$$\tilde{\theta}_{\epsilon}^{+} - \tilde{\theta}_{\epsilon}^{-} = 0 \quad \text{on } \partial D$$

$$(\nabla \tilde{\theta}_{\epsilon} \cdot \nu)^{+} - (a \nabla \tilde{\theta}_{\epsilon} \cdot \nu)^{-} = v^{(1)} \cdot \nu \quad \text{on } \partial D.$$

$$(21)$$

Notice that $\tilde{\theta}_{\epsilon}$ has oscillatory boundary data but constant coefficients, and therefore is simpler to compute than θ_{ϵ} since one no longer needs to resolve the microstructure in the interior. To use the intermediary boundary correction in the second order approximation, one could consider

$$u_{\epsilon} \approx u_0 + \epsilon \tilde{\theta}_{\epsilon} + \epsilon^2 u^{(2)} + \epsilon^2 \theta_{\epsilon}^{(2)}. \tag{22}$$

Note that $\hat{\theta}^{(2)}_{\epsilon}$ is not necessary here, as there is no difference in transmission data between θ_{ϵ} and $\tilde{\theta}_{\epsilon}$. In the numerical examples below, we demonstrate that the approximation above yields an empirical order of convergence of $O(\epsilon^3)$. One could also replace $\theta^{(2)}_{\epsilon}$ with an analogous intermediary second order boundary correction $\tilde{\theta}^{(2)}_{\epsilon}$ in the above.

We can now define the higher order modified boundary terms similarly to (12). Let $\hat{\theta}_{\epsilon}^{(i)}$ be the solution to

$$\nabla \cdot a \nabla \hat{\theta}_{\epsilon}^{(i)} + k^{2} n(x/\epsilon) \hat{\theta}_{\epsilon}^{(i)} = 0 \quad \text{in } D$$

$$\Delta \hat{\theta}_{\epsilon}^{(i)} + k^{2} \hat{\theta}_{\epsilon}^{(i)} = 0 \quad \text{in } \mathbb{R}^{d} \backslash \overline{D}$$

$$\left(\hat{\theta}_{\epsilon}^{(i)}\right)^{+} - \left(\hat{\theta}_{\epsilon}^{(i)}\right)^{-} = \left(u^{(i)} - \hat{u}^{(i)}\right) \quad \text{on } \partial D$$

$$(\nabla \hat{\theta}_{\epsilon}^{(i)} \cdot \nu)^{+} - (a \nabla \hat{\theta}_{\epsilon}^{(i)} \cdot \nu)^{-} = \left(\frac{v^{(i-1)} - \overline{v^{(i-1)}}}{\epsilon} + v^{(i)} - \overline{v}^{(i)}\right) \cdot \nu \quad \text{on } \partial D$$

$$(23)$$

with weak limit

$$\nabla \cdot a \nabla \theta^{(i)*} + k^2 \overline{n} \theta^{(i)*} = 0 \quad \text{in } D$$

$$\Delta \theta^{(i)*} + k^2 \theta^{(i)*} = 0 \quad \text{in } \mathbb{R}^d \backslash \overline{D}$$

$$(\theta^{(i)*})^+ - (\theta^{(i)*})^- = u^{(i)*} \quad \text{on } \partial D$$

$$(\nabla \theta^{(i)*} \cdot \nu)^+ - (a \nabla \theta^{(i)*} \cdot \nu)^- = (\overline{v^{(i)}}^{\partial} \cdot \nu) \quad \text{on } \partial D$$

$$(24)$$

where $u^{(i)^*}$ is the weak limit of $u^{(i)} - \hat{u}^{(i)}$, in the case of a square or a convex polygon with rational normals.

4. Convergence theorems for a square scatterer

For the second order, we show strong L^2 convergence of the boundary corrector to its limit for a sequence ϵ_m with fixed cutoff as described previously where $D=(0,1)\times(0,1)$. We prove the convergence order piece by piece, in particular, looking at the right-hand side of the square, i.e. $x_1=1$. We abuse notation a bit to set our oscillatory boundary functions to their restrictions:

$$\beta(y_2) := \beta(\delta, y_2), \quad \overline{v^{(1)}}{}^{\partial}(y_2) := \overline{v^{(1)}}{}^{\partial}(\delta, y_2).$$

We need to introduce auxiliary problems on a strip $G = G^+ \cup G^-$ where

$$G^+ = \{y_1 \ge 0; y_2 \in [0, 1]\}$$
 and $G^- = \{y_1 < 0; y_2 \in [0, 1]\}.$

Define $\Gamma := \partial D \cap \{x_1 = 1\}$ and

$$g(x/\epsilon) = a_{1i} \frac{\partial \beta}{\partial y_i} - a_{1i} \frac{\overline{\partial \beta}}{\partial y_i} \Gamma = a \nabla_y \beta(y) \cdot \nu - a (\nabla_y \beta)^*.$$

Let $\hat{w}(y_1, y_2)$ solve

$$\nabla_y \cdot a \nabla \hat{w} = 0 \qquad \text{in } G^-$$

$$\Delta_y \hat{w} = 0 \qquad \text{in } G^+$$

$$\hat{w}(0, y_2)^+ - \hat{w}(0, y_2)^- = \beta(y_2) \qquad \text{on } \partial D$$

$$\partial_{y_1} \hat{w}(0, y_2)^+ - a_{1i} \partial_{y_i} \hat{w}(0, y_2)^- = g(y_2) \qquad \text{on } \partial D$$

$$\hat{w}[0, 1] - \text{periodic in } y_2$$

There exists $\gamma > 0$ such that $e^{\pm \gamma y_1} \nabla \hat{w} \in L^2(G^{\pm})$.

Such a solution \hat{w} exists and is unique up to an additive constant across the entire strip G [12]. Because of the exponential decay of all derivatives in both directions at infinity, we have that \hat{w} approaches a constant as $y_1 \to \pm \infty$. We set

$$d^+ = \lim_{y_1 \to \infty} \hat{w}$$
 and $d^- = \lim_{y_1 \to -\infty} \hat{w}$,

and let

$$\beta^* = d^+ - d^-.$$

Later in this section, we show that β^* is the average of β on the boundary of the unit cell. Then we can similarly define w to be

$$\nabla_{y} \cdot a \nabla w = 0 \quad \text{in } G^{-}$$

$$\Delta_{y} w = 0 \quad \text{in } G^{+}$$

$$w(0, y_{2})^{+} - w(0, y_{2})^{-} = \beta(y_{2}) - \beta^{*} \quad \text{on } \partial D$$

$$\partial_{y_{1}} w(0, y_{2})^{+} - a_{1i} \partial_{y_{i}} w(0, y_{2})^{-} = g(y_{2}) \quad \text{on } \partial D$$

$$w [0, 1] - \text{periodic in } y_{2}$$
There exists $\gamma > 0$ such that $e^{\pm \gamma y_{1}} \nabla w \in L^{2}(G^{\pm})$. (26)

There exists $\gamma > 0$ such that $e^{\pm \gamma y_1} \nabla w \in L^2(G^{\pm})$. (26) For w, the additive constant can be chosen so that w itself also decays to zero as $|y_1| \to \infty$.

Proposition 4.1. Let d^+ and d^- be defined as above, i.e.

$$d^+ = \lim_{y_1 \to \infty} \hat{w}$$
 and $d^- = \lim_{y_1 \to -\infty} \hat{w}$.

We have that $\beta^* = d^+ - d^-$ is given by

$$\beta^* = \int_0^1 \beta(y_2) \, \mathrm{d}y_2.$$

Proof. From the definition of \hat{w} ,

$$\hat{w}(0, y_2)^+ - \hat{w}(0, y_2)^- = \beta(y_2).$$

We begin by considering the general Dirichlet problem. Let \hat{w}_D , periodic in y_2 , be the solution to

$$\nabla_{y} \cdot a \nabla \hat{w}_{D} = 0 \qquad y_{1} \geqslant 0, \, -\infty < y_{2} < \infty$$

$$\hat{w}_{D}(0, y_{2}) = \eta(y_{2}) \qquad -\infty < y_{2} < +\infty$$

$$e^{\gamma y_{1}} \frac{\partial \hat{w}_{D}}{\partial y_{i}} \in L^{2}(G^{+}) \quad i = 1, 2 \text{ for some } \gamma > 0$$

$$(27)$$

where $\eta(y_2)$ is extended periodically in y_2 with period [0, 1]. Let $w_D = \hat{w}_D - d$ for some constant d. Then w_D is the unique solution to

$$\nabla_{y} \cdot a \nabla w_{D} = 0 \qquad y_{1} \geqslant 0, \ -\infty < y_{2} < \infty$$

$$w_{D}(0, y_{2}) = \eta(y_{2}) - d \qquad -\infty < y_{2} < +\infty$$

$$e^{\gamma y_{1}} \frac{\partial w_{D}}{\partial y_{i}} \in L^{2}(G^{+}) \qquad i = 1, 2 \text{ for some } \gamma > 0.$$

$$(28)$$

Recall that the constant d for which w_D itself is exponentially small at $y_1 = \infty$ is given by

$$d = \int_0^1 \eta(y_2) \, \mathrm{d}y_2.$$

To see this, note from the Poincaré inequality,

$$\|\hat{w}_D(y_1,\cdot) - \overline{\hat{w}_D}(y_1)\|_{L^2(0,1)}^2 \leqslant C \left\| \frac{\partial \hat{w}_D}{\partial y_2}(y_1,\cdot) \right\|_{L^2(0,1)}^2$$

where C is independent of y_1 . For clarification, \widehat{w}_D indicates the average of \widehat{w}_D in the y_2 variable over the interval (0, 1). Multiply by $e^{2\gamma y_1}$ and integrate in y_1 over $(0, \infty)$ to get

$$\begin{split} \int_{G^+} \left(\mathrm{e}^{\gamma y_1} (\hat{w}_D(y_1, y_2) - \overline{\hat{w}_D}(y_1)) \right)^2 \mathrm{d}y_1 \, \mathrm{d}y_2 \\ &\leqslant C \! \int_{G^+} \! \left(\mathrm{e}^{\gamma y_1} \frac{\partial \hat{w}_D}{\partial y_2} \right)^2 \mathrm{d}y_1 \, \mathrm{d}y_2 < \infty. \end{split}$$

Therefore $e^{\gamma y_1}(\hat{w}_D(y_1, y_2) - \overline{\hat{w}_D}(y_1)) \in L^2(G^+)$. Note that

$$\frac{\mathrm{d}}{\mathrm{d}y_1}\overline{\widehat{w}_D}(y_1) = \frac{\mathrm{d}}{\mathrm{d}y_1}\int_0^1 \widehat{w}_D(y_1, y_2)\,\mathrm{d}y_2 = \int_0^1 \frac{\partial \widehat{w}_D}{\partial y_1}\,\mathrm{d}y_2 = 0$$

from the periodicity of \hat{w}_D . Therefore

$$\overline{\widehat{w}_D}(y_1) = \overline{\widehat{w}_D}(0) = d$$

Hence $\overline{\widehat{w}_D}(y_1) - d = 0$, and $e^{\gamma y_1}(\overline{\widehat{w}_D}(y_1) - d) \in L^2(G^+)$. Because $e^{\gamma y_1}(\widehat{w}_D(y_1, y_2) - \overline{\widehat{w}_D}(y_1)) \in L^2(G^+)$, we conclude that

$$e^{\gamma y_1} w_D = e^{\gamma y_1} (\hat{w}_D - d) \in L^2(G^+).$$

Note that -d therefore satisfies the problem on G^- .

Using this fact, and the definition of d^+ and d^- , we have

$$d^+ = \int_0^1 \hat{w}(0, y_2)^+ dy_2$$
 and $d^- = \int_0^1 \hat{w}(0, y_2)^- dy_2$.

Therefore

$$\beta^* = d^+ - d^- = \int_0^1 \left(\hat{w}(0, y_2)^+ - \hat{w}(0, y_2)^- \right) \, \mathrm{d}y_2 = \int_0^1 \beta(y_2) \, \mathrm{d}y_2.$$

With these results, we have the following convergence theorem.

Remark 4.1. In the following proof, we replace $v^{(2)} - \overline{v}^{(2)}$ by $\overline{v^{(2)}}^{\partial}$. Using the analogue of $\theta_{\epsilon} - \theta^{*}$, by lemma 5.1 in [10], we see that the piece remaining after this substitution is much like the first order boundary corrector, and so we expect the convergence order to be $O(\epsilon)$.

Theorem 4.1. (a isotropic) Let $D=(0,1)\times(0,1)$ be the unit square and let ϵ_m be a sequence approaching zero such that $\frac{1}{\epsilon_m}-\lfloor\frac{1}{\epsilon_m}\rfloor=\delta$ for all m. Let B_R be a ball of radius R>0 which contains D. Then if a is a positive constant and $\hat{\theta}^{(2)}_{\epsilon_m}$ solves (16) together with the Sommerfeld radiation condition at infinity for $\epsilon=\epsilon_m$, we have that

$$\|\hat{\theta}_{\epsilon}^{(2)} - \theta^{(2)*}\|_{L^{2}(B_{R})} \le C_{R} \epsilon^{1/2} \|u_{0}\|_{H^{1}(D)}$$

where C_R has no dependence on ϵ or u_0 and $\theta^{(2)^*}$ solves (19).

Proof. We write the beginning of the proof allowing for more general matrix a so that we can point out where we need a to be isotropic. Without loss of generality, we can assume that

the Dirichlet part of the jump data is zero in a neighborhood of the corners. If we were to only have small-support Dirichlet jumps and no Neumann jumps, the L^2 -norm would go to zero. To justify this assumption, we use the L^2 -boundedness of $\hat{\theta}_{\epsilon}^{(2)}$ which can be proven similarly to that of θ_{ϵ} in the appendix of [12]. Decompose $\hat{\theta}_{\epsilon}^{(2)}$ solving (16) into $\hat{\theta}_{\epsilon}^{(2)} = \psi_{\epsilon}^{(1)} + \psi_{\epsilon}^{(2)}$ where $\psi_{\epsilon}^{(1)}$ satisfies

$$\nabla \cdot a \nabla \psi_{\epsilon}^{(1)} + k^{2} n(x/\epsilon) \psi_{\epsilon}^{(1)} = 0 \quad \text{in } D$$

$$\Delta \psi_{\epsilon}^{(1)} + k^{2} \psi_{\epsilon}^{(1)} = 0 \quad \text{in } \mathbb{R}^{2} \backslash \overline{D}$$

$$\left(\psi_{\epsilon}^{(1)}\right)^{+} - \left(\psi_{\epsilon}^{(1)}\right)^{-} = 1_{x_{1}=1} k^{2} \beta^{*} u_{0}(x) \quad \text{on } \partial D$$

$$(\nabla \psi_{\epsilon}^{(1)} \cdot \nu)^{+} - (a \nabla \psi_{\epsilon}^{(1)} \cdot \nu)^{-} = 1_{x_{1}=1} \left(\overline{v^{(2)}} \partial \cdot \nu\right) \quad \text{on } \partial D$$

$$(29)$$

and $\psi_{\epsilon}^{(2)}$ solves

$$\nabla \cdot a \nabla \psi_{\epsilon}^{(2)} + k^{2} n(x/\epsilon) \psi_{\epsilon}^{(2)} = 0 \quad \text{in } D$$

$$\Delta \psi_{\epsilon}^{(2)} + k^{2} \psi_{\epsilon}^{(2)} = 0 \quad \text{in } \mathbb{R}^{2} \backslash \overline{D}$$

$$(\psi_{\epsilon}^{(2)})^{+} - (\psi_{\epsilon}^{(2)})^{-} = 1_{x_{1}=1} k^{2} (\beta(x/\epsilon) - \beta^{*}) u_{0}(x) \quad \text{on } \partial D$$

$$(\nabla \psi_{\epsilon}^{(2)} \cdot \nu)^{+} - (a \nabla \psi_{\epsilon}^{(2)} \cdot \nu)^{-} = 1_{x_{1}=1} \epsilon^{-1} g(x/\epsilon) u_{0}(x) \quad \text{on } \partial D$$

$$(30)$$

complemented with the Sommerfeld radiation condition at infinity. By homogenization theory in the first order, we have that

$$\|\psi_{\epsilon}^{(1)} - \theta^{(2)*}\|_{L^2(B_R)} \leqslant C_R \epsilon.$$

Define $V(x_2)$ to be the restriction of $u_0(x)$ to $\partial D \cap \{x_1 = 1\}$, extended as a constant in the x_1 -direction and extended by zero for x_2 outside of (0,1). By our earlier assumption, we have that $V(x_2)$ is zero in a neighborhood of $x_2 = 0$, 1, so that this extension is smooth. Define $\phi(x_1)$ to be a smooth cutoff function (constant in x_2) such that $\phi \equiv 1$ for $x_1 \geqslant 1$ and $\phi \equiv 0$ for $x_1 \leqslant 0$. Let

$$\psi_{\epsilon}^{(3)} = w\left(\frac{x_1 - 1}{\epsilon}, \frac{x_2}{\epsilon}\right)$$

where w solves (25) with constant chosen so that w goes to zero as $y_1 \to \pm \infty$. Set

$$\psi_{\epsilon}^{(4)} = \psi_{\epsilon}^{(3)} V(x_2) \phi(x_1).$$

Using the triangle inequality, we can bound $\psi_{\epsilon}^{(2)}$ in $L_{loc}^2(\mathbb{R}^2)$ by

$$\|\psi_{\epsilon}^{(2)}\|_{L^{2}(B_{R})} \leqslant \|\psi_{\epsilon}^{(2)} - \psi_{\epsilon}^{(4)}\|_{L^{2}(B_{R})} + \|\psi_{\epsilon}^{(4)}\|_{L^{2}(B_{R})}.$$

Because of the way w was defined, there exists $\gamma > 0$ such that $e^{\pm \gamma y_1} \nabla w \in L^2(G^{\pm})$. By definition of $\psi_{\epsilon}^{(4)}$, we have

$$|\psi_{\epsilon}^{(4)}| \leqslant Ce^{-\gamma \frac{|x_1-1|}{\epsilon}} ||u_0||_{H^1(D)}.$$

Let $\Phi \in C_0^{\infty}(D)$ be any test function. For fixed $0 < x_2 < 1$, integrating by parts and using the weak derivative of $|\Phi|$, we have

$$\int_0^1 \exp\left(\gamma \frac{x_1 - 1}{\epsilon}\right) |\Phi| \, \mathrm{d}x_1 \leqslant C\epsilon \left(\int_0^1 \left| \frac{\partial}{\partial x_1} \Phi(x_1, x_2) \right|^2 \mathrm{d}x_1 \right)^{1/2}.$$

Therefore we have

$$\|\psi_{\epsilon}^{(4)}\|_{L^2(B_R)} \leqslant C\epsilon \|u_0\|_{H^1(D)}.$$

By definition of $\psi_{\epsilon}^{(2)}$ and $\psi_{\epsilon}^{(4)}$, the residual $\psi_{\epsilon}^{(2)} - \psi_{\epsilon}^{(4)}$ solves

$$\begin{split} \nabla \cdot a \nabla \left(\psi_{\epsilon}^{(2)} - \psi_{\epsilon}^{(4)} \right) + k^2 n(x/\epsilon) \left(\psi_{\epsilon}^{(2)} - \psi_{\epsilon}^{(4)} \right) \\ &= -2a \nabla \psi_{\epsilon}^{(3)} \cdot \nabla V \phi - \psi_{\epsilon}^{(3)} a : \nabla \nabla (V \phi) - k^2 n \psi_{\epsilon}^{(3)} V \phi \quad \text{in } D \end{split}$$

$$\begin{split} &\Delta \left(\psi_{\epsilon}^{(2)} - \psi_{\epsilon}^{(4)} \right) + k^2 \left(\psi_{\epsilon}^{(2)} - \psi_{\epsilon}^{(4)} \right) \\ &= -2 \nabla \psi_{\epsilon}^{(3)} \cdot \nabla V \phi - \psi_{\epsilon}^{(3)} \Delta (V \phi) - k^2 \psi_{\epsilon}^{(3)} V \phi \quad \text{in } \mathbb{R}^2 \backslash \overline{D} \end{split}$$

$$(\psi_{\epsilon}^{(2)} - \psi_{\epsilon}^{(4)})^{+} - (\psi_{\epsilon}^{(2)} - \psi_{\epsilon}^{(4)})^{-} = 0 \qquad \text{on } \partial D$$

$$\nabla (\psi_{\epsilon}^{(2)} - \psi_{\epsilon}^{(4)})^{+} \cdot \nu - a \nabla (\psi_{\epsilon}^{(2)} - \psi_{\epsilon}^{(4)})^{-} \cdot \nu = -a_{12} w^{-} V'(x_{2}) \qquad \text{on } \partial D.$$
(31)

It is at this point we need to assume that a is a scalar constant, which makes the above conormal residual jump equal to zero. With $\Phi \in C_0^{\infty}(D)$, using integration by parts we then have

$$\begin{split} \left| \int_{D} \psi_{\epsilon}^{(3)} a \Delta(V\phi) \Phi \, \mathrm{d}x \right| & \leq \left| \int_{D} a \nabla \psi_{\epsilon}^{(3)} \cdot \nabla (V\phi) \Phi \, \mathrm{d}x \right| \\ & + \left| \int_{\partial D} a \nabla (V\phi) \cdot \nu \, \psi_{\epsilon}^{(3)} \Phi \, \mathrm{d}x \right| = \left| \int_{D} a \nabla \psi_{\epsilon}^{(3)} \cdot \nabla (V\phi) \Phi \, \mathrm{d}x \right|. \end{split}$$

Therefore we can find a bound for the right-hand side term of the partial differential equation that the residual solves inside *D* by looking at the bound of

$$\left| a \nabla \psi_{\epsilon}^{(3)} \cdot \nabla (V\phi) + k^2 n(x/\epsilon) \psi_{\epsilon}^{(3)} V\phi \right|.$$

As before, due to the exponential decay of w, we have

$$|\nabla \psi_{\epsilon}^{(3)}| \leqslant |\nabla w| \leqslant \epsilon^{-1} |\nabla_{y} w| \leqslant \frac{C}{\epsilon} e^{-\gamma \frac{|x_{1}-1|}{\epsilon}}.$$

Therefore we have

$$\left| \int_{D} a \nabla \psi_{\epsilon}^{(3)} \cdot \nabla (V\phi) \, \Phi \, \mathrm{d}x \right| \leqslant \frac{C}{\epsilon} \int_{D} \exp \left(\gamma \frac{x_{1} - 1}{\epsilon} \right) \, |\nabla (V\phi)| \, |\Phi| \, \mathrm{d}x.$$

Because $\nabla(V\phi)$ is bounded in D, we must have that

$$\left| \int_D a \nabla \psi_\epsilon^{(3)} \cdot \nabla (V\phi) \, \Phi \, \mathrm{d}x \right| \leqslant C \int_D \frac{1}{\epsilon} \exp \left(\gamma \frac{x_1 - 1}{\epsilon} \right) \, |\Phi| \, \mathrm{d}x.$$

Similarly to before, for fixed $0 < x_2 < 1$, we have that

$$\int_0^1 \frac{1}{\epsilon} \exp\left(\gamma \frac{x_1 - 1}{\epsilon}\right) \left| \Phi \right| \mathrm{d}x_1 \leqslant C \epsilon^{1/2} \left(\int_0^1 \left| \frac{\partial}{\partial x_1} \Phi(x_1, x_2) \right|^2 \mathrm{d}x_1 \right)^{1/2}.$$

Integrating the above over x_2 and using the Cauchy–Schwartz inequality again, we have

$$\int_{D} \frac{1}{\epsilon} \exp\left(\gamma \frac{x_1 - 1}{\epsilon}\right) |\Phi| \, \mathrm{d}x \leqslant C \epsilon^{1/2} \|\Phi\|_{H_0^1(D)}.$$

Therefore

$$||a\nabla\psi_{\epsilon}^{(3)}\cdot\nabla(V\phi)||_{H^{-1}(D)}\leqslant C\epsilon^{1/2}.$$

Moreover, using the fact that $n \in C^{\infty}(D)$, we have

$$||k^2 n(x/\epsilon)\psi_{\epsilon}^{(3)}V\phi||_{L^2(B_R)} \le C\epsilon ||u_0||_{H^1(D)}.$$

Therefore we can bound the data for the residual inside D by $C\epsilon^{1/2}\|u_0\|_{H^1(D)}$. We can bound the data for the residual outside of D similarly. Thus we have shown that

$$\|\psi_{\epsilon}^{(2)}\|_{L^{2}(B_{R})} \leq \|\psi_{\epsilon}^{(2)} - \psi_{\epsilon}^{(4)}\|_{L^{2}(B_{R})} + \|\psi_{\epsilon}^{(4)}\|_{L^{2}(B_{R})}$$

$$\leq C\epsilon^{1/2} \|u_{0}\|_{H^{1}(D)} + C\epsilon \|u_{0}\|_{H^{1}(D)}$$

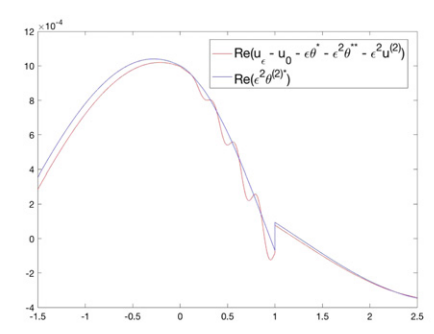
$$\leq C\epsilon^{1/2} \|u_{0}\|_{H^{1}(D)}$$

which completes the proof.

Remark 4.2. Note that any domain which has a flat boundary portion with rational normal will yield a nonzero limit, and therefore the above theorems hold for such a domain in general for the piece of $\hat{\theta}_{\epsilon}^{(2)}$ which lives on the flat part. For the case when a is anisotropic, the residual $\psi_{\epsilon}^{(2)} - \psi_{\epsilon}^{(4)}$ has nonzero conormal jump in (31). In this case one can show that the convergence satisfies

$$\|\hat{\theta}_{\epsilon}^{(2)} - \theta^{(2)*}\|_{L^{2}(R_{P})} \leqslant C_{R} \epsilon^{1/2} (\|u_{0}\|_{H^{1}(\partial D)} + \|u_{0}\|_{H^{1}(D)}). \tag{32}$$

Unfortunately, in the case of a polygon, one may not always have u_0 in $H^1(\partial D)$. However, for a smooth domain which has a flat boundary portion with rational normal or for certain choices for matrix a one may have u_0 in $H^{3/2}(D)$, and therefore we include the above estimate in this remark. Note that for the case of a general domain with flat boundary portion, one would need to use a change of variables to translate to the side of a square.



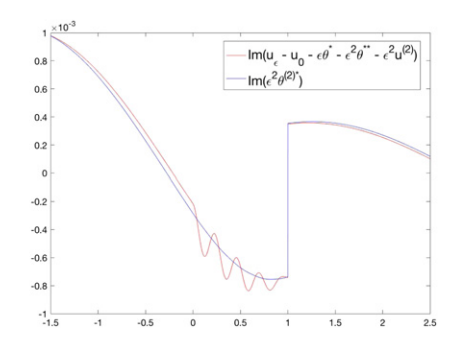
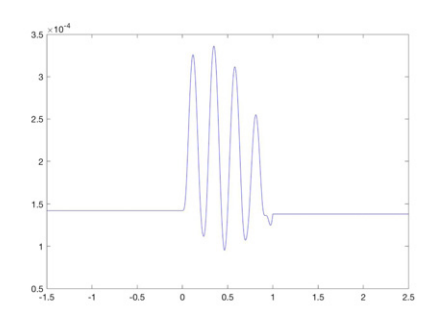
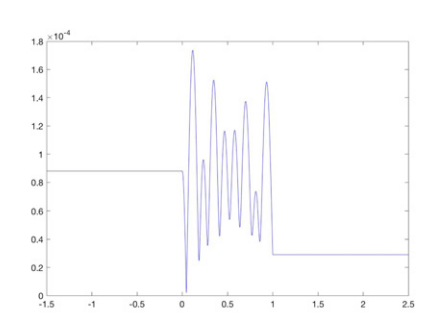


Figure 1. Real (left) and imaginary (right) parts of the error $u_{\epsilon} - (u_0 + \epsilon \theta^* + \epsilon^2 \theta^{**} + \epsilon^2 u^{(2)})$ (red) vs second order limiting boundary corrector $\epsilon^2 \theta^{(2)^*}$ (blue) assuming $n(y) = 2 + \sin(2\pi y)$ and $\epsilon = 1/4.\overline{3}$, k = 1. The scatterer D is defined to be (0, 1), and we plot both inside and outside of the scatterer for $x \in (-1.5, 2.5)$.





- (a) Oscillatory Boundary Correctors
- (b) Limiting Boundary Correctors

Figure 2. Absolute error between u_{ϵ} and second order approximations with oscillatory boundary correctors as in (7) (left) and limiting boundary correctors as in (20) (right) assuming $n(y) = 2 + \sin(2\pi y)$ and $\epsilon = 1/4.\overline{3}$, k = 1. Note that the order of error is the same for both approximations. The scatterer D is defined to be (0,1), and we plot both inside and outside of the scatterer for $x \in (-1.5, 2.5)$.

5. One dimensional problem

We now study numerically the use of the limiting second order approximation proposed in (20). Using this approximation, we observed an empirical order of convergence of $O(\epsilon^3)$, in the case where the periodic scattering media occupies the interval (0, 1). We include plots of the real and imaginary parts of $\epsilon^2\theta^{(2)^*}$ alongside the real and imaginary parts of the error between u_{ϵ} and $u_0 + \epsilon \theta^* + \epsilon^2 \theta^{**} + \epsilon^2 u^{(2)}$ for $\epsilon = 1/4.\overline{3}$ in figure 1. Note that $\epsilon^2\theta^{(2)^*}$ is sufficient to act as the second order boundary corrector in both the domain and the exterior field. In figure 2 we show that the order of absolute error is the same using oscillatory boundary correctors as in the second order approximation (7) vs using limiting boundary correctors as in (20).

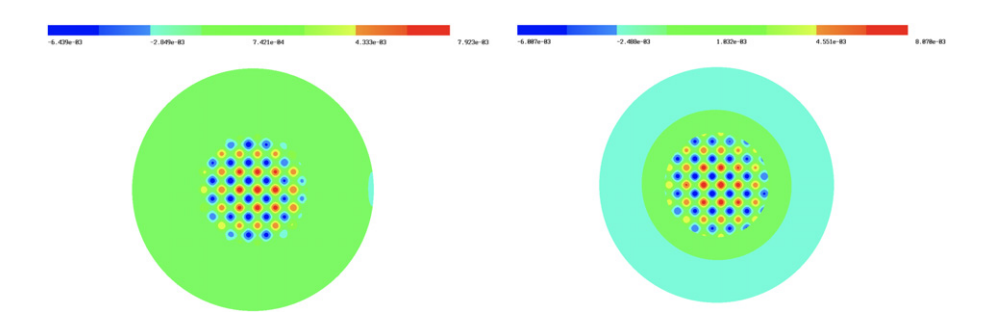


Figure 3. Circular domain with smooth n(y) given by (33). Contour plots of $u_{\epsilon} - u_0 - \epsilon \theta_{\epsilon}$ (left) vs $\epsilon^2 u^{(2)}$ (right) assuming $\epsilon = 1/3$ and k = 1. Note that the PML region begins at r = 1.75.

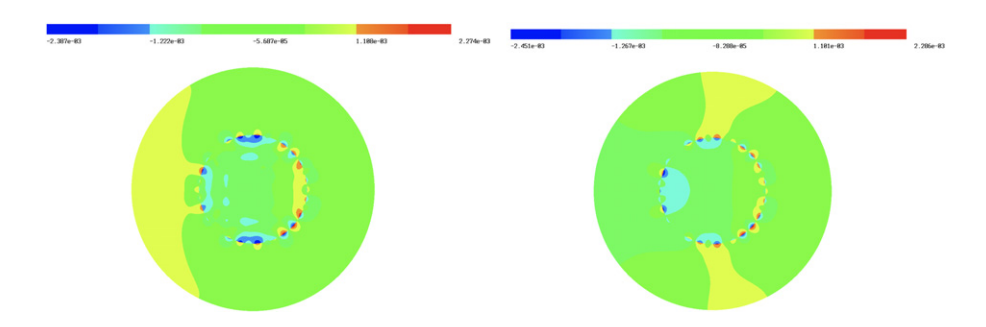


Figure 4. Circular domain with smooth n(y) given by (33). Contour plots of $u_{\epsilon} - u_0 - \epsilon \theta_{\epsilon} - \epsilon^2 u^{(2)}$ (left) vs $\epsilon^2 \theta_{\epsilon}^{(2)}$ (right) assuming $\epsilon = 1/3$ and k = 1. Note that the PML region begins at r = 1.75.

6. Two dimensional problem

6.1. Circular domain

We first consider a smoothly varying n. Let D be the circle of radius 1 centered at the origin, a = I (the identity), and consider the true solution u_{ϵ} with

$$n(y) = 2 + \sin(2\pi y_1) + \cos(2\pi y_2). \tag{33}$$

Assume the incident wave u_i is given by $\mathrm{e}^{\mathrm{i}k(\cos\theta x_1+\sin\theta x_2)}$ for some $\theta\in[0,2\pi)$. The following numerical computations are performed in the open source finite element package Netgen/NGSolve [36]. We numerically compute the scattered solution u_s using cubic finite elements with radial perfectly matched layers to model the radiation boundary conditions. The scattered field of the homogenized solution can be computed similarly. Since the limiting boundary correctors for a smooth domain with no flat parts are zero, we compute θ_ϵ , $\hat{u}^{(2)}$, and $\theta_\epsilon^{(2)}$ using the same methodology.

Numerical results in figure 3 show that $\epsilon^2 u^{(2)}$ corrects for the oscillatory behavior remaining in the bulk after the addition of $\epsilon\theta_{\epsilon}$ as described in the theory. Moreover, figure 4 shows that $\epsilon^2\theta_{\epsilon}^{(2)}$ corrects both in the domain and in the far field. In figure 5 we plot $\log_2(\epsilon)$ vs $\log_{10}(E)$ where E is the error in the L^2 -norm for the varying approximations. The slope α is the observed order of convergence $O(\epsilon^{\alpha})$. Note that the empirical order of convergence α which we are

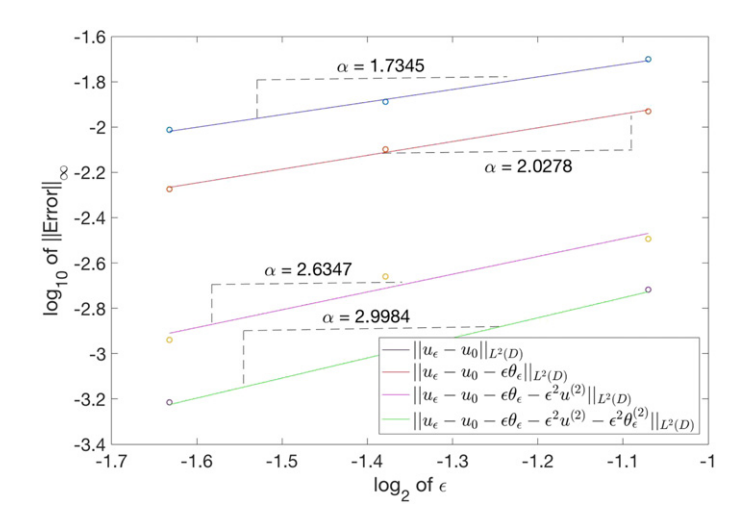


Figure 5. Circular domain with smooth n(y) given by (33). Log-log plot showing the observed convergence ϵ^{α} : error without boundary correction (blue), error with first boundary correction $\epsilon\theta_{\epsilon}$ (red), error with first order boundary correction and second order bulk correction $\epsilon\theta_{\epsilon} + \epsilon^2 u^{(2)}$ (pink), error with second order bulk correction and first and second order boundary correction $\epsilon\theta_{\epsilon} + \epsilon^2 u^{(2)} + \epsilon^2 \theta_{\epsilon}^{(2)}$ (green), $\epsilon = 1/2.1$, 1/2.6, and 1/3.1.

observing for the rate at which $\theta_{\epsilon}^{(2)}$ is converging to its limit $\theta^{(2)^*} = 0$ is 0.695 449. Replacing $\tilde{\theta}_{\epsilon}$ with θ_{ϵ} yields similar numerical results.

6.2. Square domain

We now consider a smoothly varying periodic n on a square. Let $D = (0, 1) \times (0, 1)$, a = I (the identity), and consider the true solution u_{ϵ} with $n(y) = n(y_1) = 2 + \sin(2\pi y_1)$.

Recall the second order approximation with first order limiting boundary correction given in (18) as

$$u_{\epsilon} = u_0 + \epsilon \theta^* + \epsilon^2 \theta^{**} + \epsilon^2 u^{(2)} + \epsilon^2 \hat{\theta}_{\epsilon}^{(2)} + o(\epsilon^2).$$

We numerically compute the true solution as before as well as the approximation above and observe an empirical order of convergence of $O(\epsilon^3)$. In figure 6, one sees that $\epsilon^2 u^{(2)}$ corrects for the oscillatory behavior remaining in the bulk after the addition of $\epsilon\theta^* + \epsilon^2\theta^{**}$. Furthermore, numerical results in figure 7 show that $\epsilon^2\hat{\theta}^{(2)}_{\epsilon}$ acts to correct the remaining error noticeable at the boundary of D. In figure 8, we show that the difference between $\hat{\theta}^{(2)}_{\epsilon}$ and $\theta^{(2)^*}$ contains only oscillations as $\theta^{(2)^*}$ is a subsequential limit with no oscillatory behavior. We also include a log-log plot of the empirical order of convergence of $\hat{\theta}^{(2)}_{\epsilon}$ to $\theta^{(2)^*}$ for different cutoffs of ϵ . Note that we are observing $O(\epsilon^{1/2})$ convergence as seen in the theory.

6.3. Exterior field expansion and inversion

We investigate the use of the expansion

$$u_{\epsilon}(x) \approx u_0 + \epsilon \theta_{\epsilon}$$

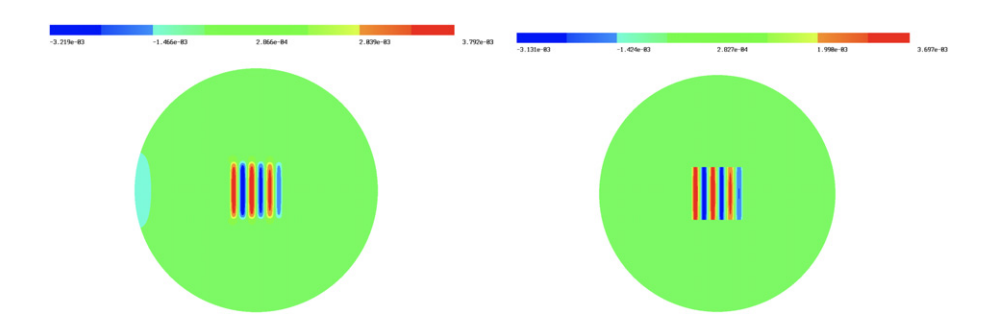


Figure 6. Square domain with smooth $n(y) = 2 + \sin(2\pi y_1)$. Contour plots of $u_{\epsilon} - u_0 - \epsilon \theta^* - \epsilon^2 \theta^{**}$ (left) vs $\epsilon^2 u^{(2)}$ (right) assuming $\epsilon = 1/3$ and k = 1. Note that the PML region begins at the circle centered at (0.5, 0.5) with radius 1.75.

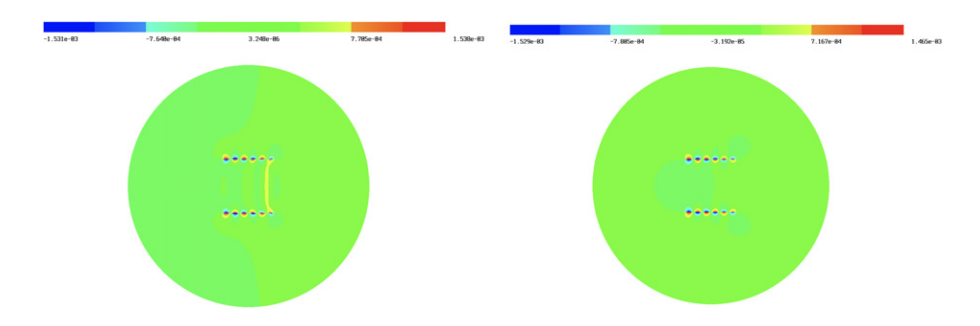


Figure 7. Square domain with smooth $n(y) = 2 + \sin(2\pi y_1)$. Contour plots of $u_{\epsilon} - u_0 - \epsilon \theta^* - \epsilon^2 \theta^{**} - \epsilon^2 u^{(2)}$ (left) vs $\epsilon^2 \hat{\theta}_{\epsilon}^{(2)}$ (right) assuming $\epsilon = 1/3$ and k = 1. Note that the PML region begins at the circle centered at (0.5, 0.5) with radius 1.75.

as a model for exterior field measurements to recover properties of n(x). Let us assume that one can read the solution u_{ϵ} in the far field. Recall the first order approximation for u_{ϵ} , that is,

$$u_{\epsilon} \approx u_0 + \epsilon \tilde{\theta}_{\epsilon},$$

where $\tilde{\theta}_{\epsilon}$ solves (8) with \overline{n} in place of $n(x/\epsilon)$. From [10], we can write $\tilde{\theta}_{\epsilon}$ as the single layer potential

$$\tilde{\theta}_{\epsilon}(z) = k^2 \int_{\partial D} a \nabla_{y} \beta(x/\epsilon) \cdot \nu \, u_0(x) G^{a,\overline{n}}(z,x) \, d\sigma_{x}$$

where $G^{a,\overline{n}}$ is the fundamental solution corresponding to a background with the homogenized scatterer embedded. Using integration by parts and because $\nabla_y \cdot a \nabla_y \beta = \overline{n} - n$, we have the following approximation in the exterior field

$$u_{\epsilon}(z) \approx u_{0}(z) + \epsilon \tilde{\theta}_{\epsilon}(z)$$

$$\approx u_{0}(z) + k^{2} \int_{D} (\overline{n} - n(x/\epsilon)) u_{0}(x) G^{a,\overline{n}}(z,x) dx + O(\epsilon^{2}).$$
(34)

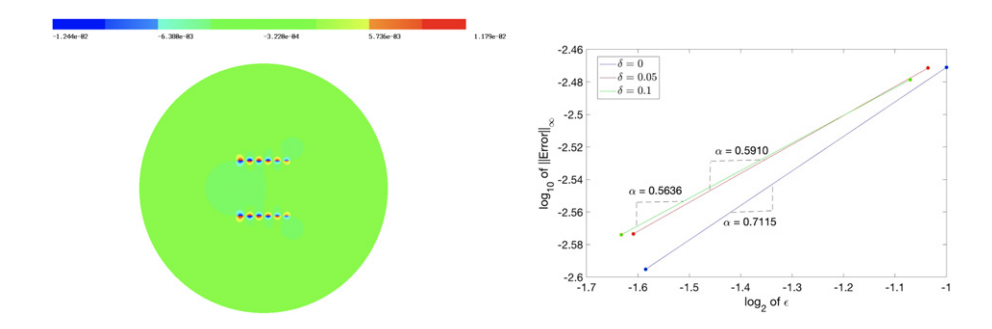


Figure 8. Square domain with smooth $n(y) = 2 + \sin(2\pi y_1)$. On the left, contour plot of $\hat{\theta}_{\epsilon}^{(2)} - \theta^{(2)*}$ (right) assuming $\epsilon = 1/3$ and k = 1. Note that the PML region begins at the circle centered at (0.5, 0.5) with radius 1.75. On the right, log-log plot showing the observed convergence ϵ^{α} : error of $\hat{\theta}_{\epsilon}^{(2)} - \theta^{(2)*}$ for different cutoffs δ .

Assuming one knows the location of the scatterer D, the constant a, the average \overline{n} , ϵ , and can control the incident wave, one can use the above expansion to recover an approximation of $n(x/\epsilon)$ as a finite sum of smooth periodic elements.

One may also use the second order e^2 terms to model the far field information,

$$u_{\epsilon} \approx u_0 + \epsilon \tilde{\theta}_{\epsilon} + \epsilon^2 \theta^{**} + \epsilon^2 \hat{u}^{(2)} + \epsilon^2 \tilde{\theta}_{\epsilon}^{(2)} + O(\epsilon^3),$$
 (35)

which could be used to recover $\overline{n\beta}$ and $\nabla_y \beta$. One can write the second order bulk correction $\hat{u}^{(2)}$ using the fundamental solution

$$\hat{u}^{(2)}(z) = -k^4 \overline{n\beta} \int_D u_0(x) G^{a,\overline{n}}(z,x) \,\mathrm{d}x,\tag{36}$$

and similarly, using integration by parts, the second order boundary corrector $\tilde{\theta}^{(2)}_{\epsilon}$ can be written using layer potentials

$$\begin{split} \tilde{\theta}_{\epsilon}^{(2)}(z) &= \frac{k^2}{\epsilon} \int_D (\nabla_y \beta \cdot \nabla_x G^{a,\overline{n}}) u_0(x) \, \mathrm{d}x + k^2 \int_D (\nabla_x u_0 \cdot \nabla_x G^{a,\overline{n}}) \beta(x/\epsilon) \, \mathrm{d}x \\ &+ k^2 \int_D \beta(x/\epsilon) u_0(x) \Delta G^{a,\overline{n}}(z,x) \, \mathrm{d}x + \frac{k^2}{\epsilon} \int_D \nabla_x (u_0 G^{a,\overline{n}}) \cdot (a \nabla_y \beta) \, \mathrm{d}x \\ &+ \frac{k^2}{\epsilon^2} \int_D (\nabla_y \cdot a \nabla_y \beta) u_0(x) G^{a,\overline{n}}(z,x) \, \mathrm{d}x - \frac{k^2}{\epsilon} \int_{\partial D} \left(a \nabla_y \beta^* \cdot \nu \right) u_0(x) G^{a,\overline{n}}(z,x) \mathrm{d}\sigma_x \\ &- k^2 \int_{\partial D} \beta^* (a \nabla u_0 \cdot \nu) G^{a,\overline{n}}(z,x) \mathrm{d}\sigma_x. \end{split}$$

Plugging this into (35) along with (36), we derive the second order far field approximation for a general domain to be

$$\begin{split} u_{\epsilon}(z) &\approx u_{0}(z) + k^{2} \int_{D} (\overline{n} - n(x/\epsilon)) u_{0}(x) G^{a,\overline{n}}(z,x) \, \mathrm{d}x \\ &+ 2\epsilon k^{2} \int_{D} a \nabla_{y} \beta(x/\epsilon) \cdot \nabla_{x} (u_{0}(x) G^{a,\overline{n}}(z,x)) \, \mathrm{d}x \\ &+ \epsilon k^{2} \int_{\partial D} \left[\left(\nabla_{y} \beta \cdot \nu \right) - \left(a \nabla_{y} \beta \cdot \nu \right)^{*} \right] \, u_{0}(x) G^{a,\overline{n}}(z,x) \, \mathrm{d}\sigma_{x} \\ &+ \epsilon k^{2} \int_{D} (\overline{n} - n(x/\epsilon)) \theta^{*} G^{a,\overline{n}} \, \mathrm{d}x - \epsilon^{2} k^{4} \overline{n\beta} \int_{D} u_{0}(x) G^{a,\overline{n}}(z,x) \, \mathrm{d}x \\ &- \epsilon^{2} k^{2} \int_{\partial D} \beta^{*} \left(a \nabla u_{0}(x) \cdot \nu \right) G^{a,\overline{n}}(z,x) \, \mathrm{d}\sigma_{x} + O(\epsilon^{3}). \end{split}$$

For smooth domains with no flat parts, we have that $\beta^* = 0$, and hence the approximation above can be simplified to

$$u_{\epsilon}(z) \approx u_{0}(z) + k^{2} \int_{D} (\overline{n} - n(x/\epsilon)) u_{0}(x) G^{a,\overline{n}}(z,x) \, \mathrm{d}x$$

$$+ 2\epsilon k^{2} \int_{D} a \nabla_{y} \beta(x/\epsilon) \cdot \nabla_{x} (u_{0}(x) G^{a,\overline{n}}(z,x)) \, \mathrm{d}x$$

$$+ \epsilon k^{2} \int_{\partial D} (\nabla_{y} \beta \cdot \nu) \cdot \nu \, u_{0}(x) G^{a,\overline{n}}(z,x) \, \mathrm{d}\sigma_{x}$$

$$- \epsilon^{2} k^{4} \overline{n\beta} \int_{D} u_{0}(x) G^{a,\overline{n}}(z,x) \, \mathrm{d}x + O(\epsilon^{3}).$$

For the following numerical experiments, we use (34) to recover properties of n(x). The techniques presented are implemented in the open source finite element package Netgen/NGSolve [36].

6.3.1. Smooth n. We first consider a smoothly varying periodic n on a circle. Let D be the circle of radius 1 centered at (0,0), a=I (the identity), and consider the solution u_{ϵ} with (33). Assume the incident wave u_i is given by $e^{ik(\cos\theta x_1 + \sin\theta x_2)}$. We simulate data outside the scatterer by numerically computing the true solution and the homogenized solution using cubic finite elements with radial perfectly matched layers to model the radiation boundary conditions. We read $(u_{\epsilon} - u_0)(z)$ at K equidistant points $z \in \mathbb{R}^2$ lying on the circle of radius 1.99 centered at (0,0). We repeat this procedure for N incident waves by varying θ in the incident wave. The Green's function $G^{a,\overline{n}}(z,x)$ is computed using cubic finite elements with perfectly matched layers for each z_1,\ldots,z_K . In order to estimate the delta function, we use a Gaussian,

$$\delta(x,y) = \lim_{\sigma \to 0} \frac{1}{2\pi\sigma^2} e^{-((x-z_1)^2 + (y-z_2)^2)/(2\sigma^2)}, \quad z = (z_1, z_2)$$
(37)

with $\sigma=1/59$. We then use a basis of M smooth periodic elements to approximate n(x), that is, $n(x/\epsilon) \approx \overline{n} + \sum_{j=1}^{M} c_j \phi_j(x/\epsilon)$, and solve for the unknown coefficients in

$$u_{\epsilon}(z) - u_0(z) \approx -k^2 \sum_{i=1}^{M} c_j \int_{D} \phi_j(x/\epsilon) u_0(x) G^{a,\overline{h}}(z,x) \,\mathrm{d}x. \tag{38}$$

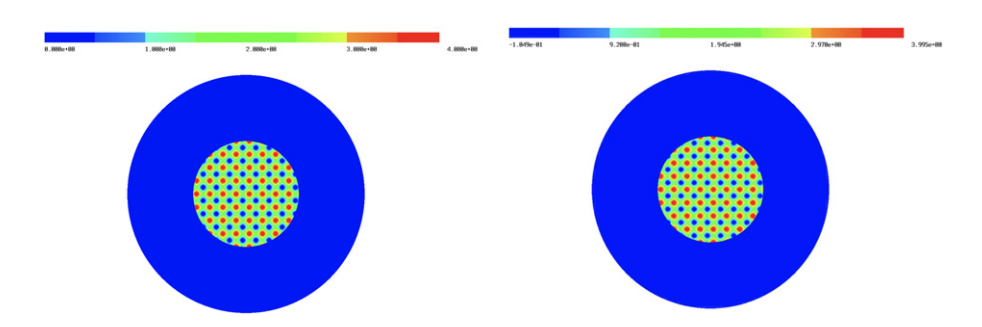


Figure 9. Results of numerical inversion with $n(x/\epsilon)$ given by (33) (left) and recovered n (right) plotted on the circular scatterer D with radius r=1, $\epsilon=1/4$. Data is read in the exterior field at a radius of r=1.99.

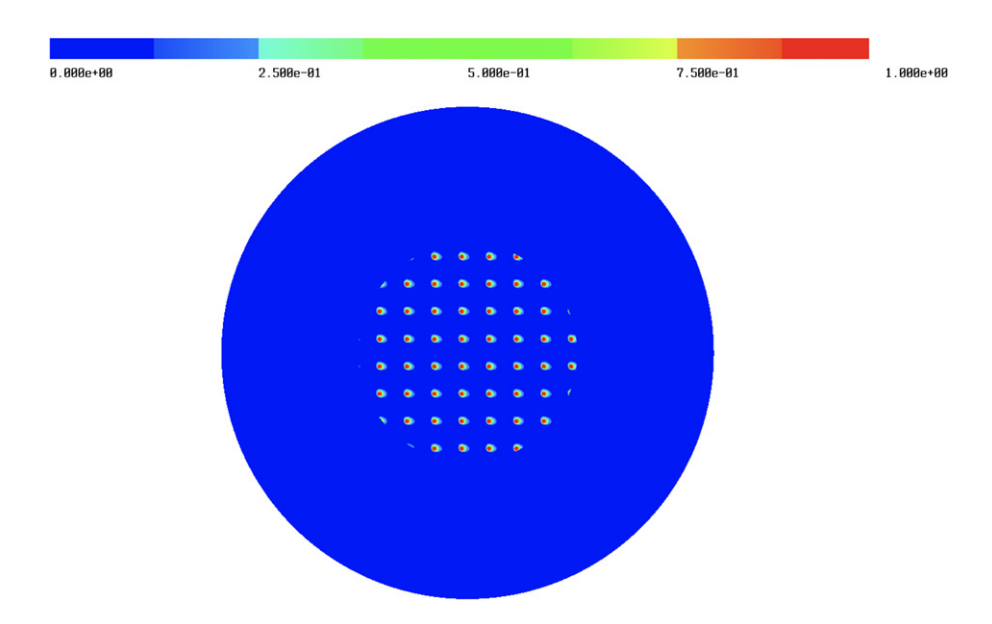


Figure 10. Relative error between $n(x/\epsilon)$ given by (33) and recovered n given in figure 9.

As the system we create is of coursed ill-posed, hence we solve the regularized least-squares problem

$$\min \|b - Ax\|_2^2 + \alpha \|x\|_2^2$$

where α is the regularization strength. Numerical results in figure 9 show that the first order approximation of the exterior field given in (34) allows us to recover qualitative properties of n(x). In figure 10, we plot the relative error between the true $n(x/\epsilon)$ given by (33) and the recovered n. The L^1 norm of the relative error is $0.000\,582\,83$.

For results in figure 9, we use N=3 incident waves, K=3 equidistant points, and M=9 smooth periodic elements, as our true n(y) lies within our test space. For this example, we also consider imperfect data by introducing 1%, 5%, and 10% noise to the data. We use a Gaussian with zero mean and standard deviation 1 to model the noise. In figure 11, we observe

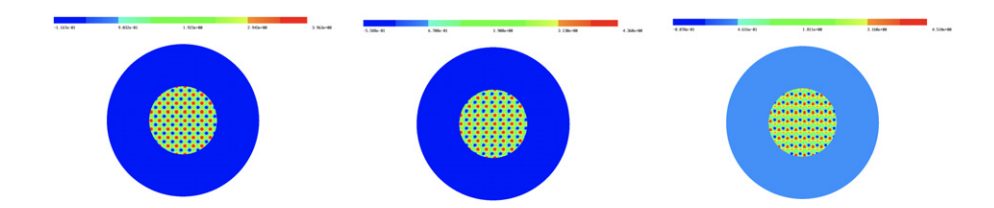


Figure 11. Results of numerical inversion with $n(y) = 2 + \sin(2\pi y_1) + \cos(2\pi y_2)$ and recovered n with noise, circular scatterer D with radius r = 1, $\epsilon = 1/4$. From left to right: percentage of noise is 1%, 5%, and 10%. Data is read in the exterior field at a radius of r = 1.99.

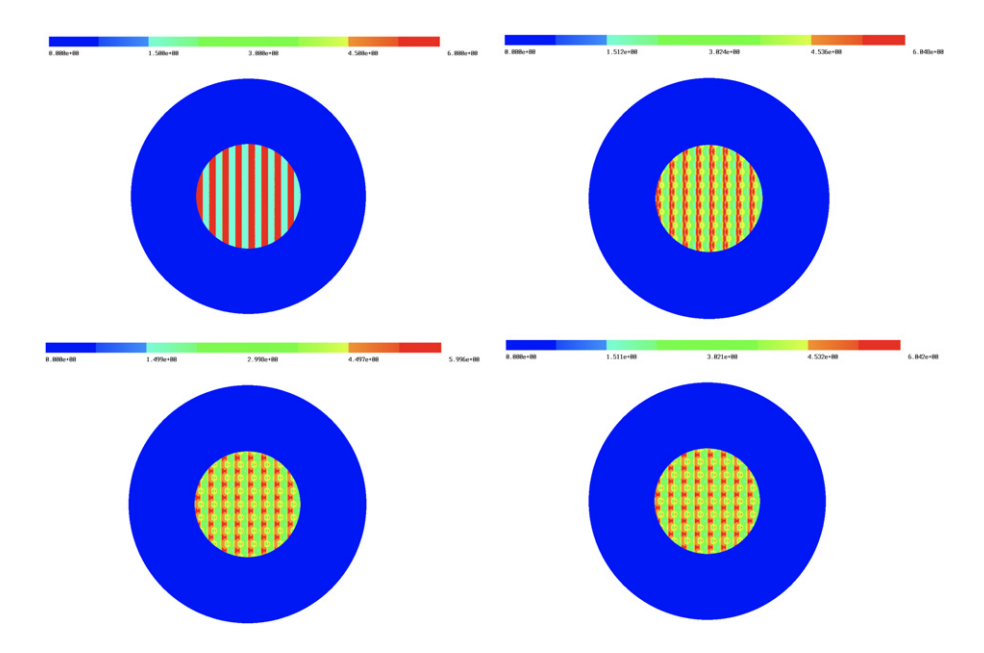


Figure 12. Inversion with $n(x/\epsilon)$ given by (39) and recovered n for the circular scatterer D of radius 1, $\epsilon = 1/4$. Top left: true solution n, top right: recovered n reading data in the exterior field on the circle r = 1.1, bottom left: recovered n reading data at r = 1.5, bottom right: recovered n reading data at r = 1.99.

a relatively accurate approximation for n(x) for small noise. As the noise grows, our recovery of n deteriorates.

6.3.2. Piecewise constant layering. Let D again be the unit circle. In this example, we choose a piecewise-constant periodic n(y) with high contrast,

$$n(y) = \begin{cases} 6 & y_1 \in [0, 0.5) \\ 2 & y_1 \in [0.5, 1). \end{cases}$$
 (39)

We again assume we know ϵ , the location of the scatterer D, and that the interior of the scatterer has a periodic structure by modeling n using two-dimensional, smoothly varying periodic elements. Again, we see that the first order approximation of the far field allows us to recover

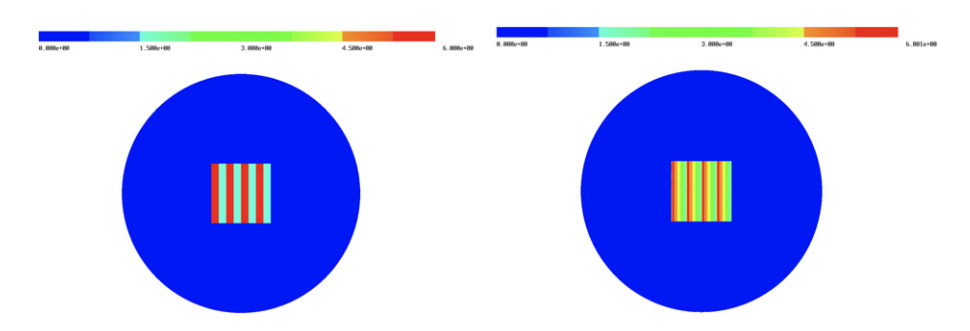


Figure 13. Results of numerical inversion with $n(x/\epsilon)$ given by (39) (left) and recovered n (right) for the square scatterer $D=(-0.5,-0.5)\times(0.5,0.5), \epsilon=1/4$. Data is read at a radius of r=1.

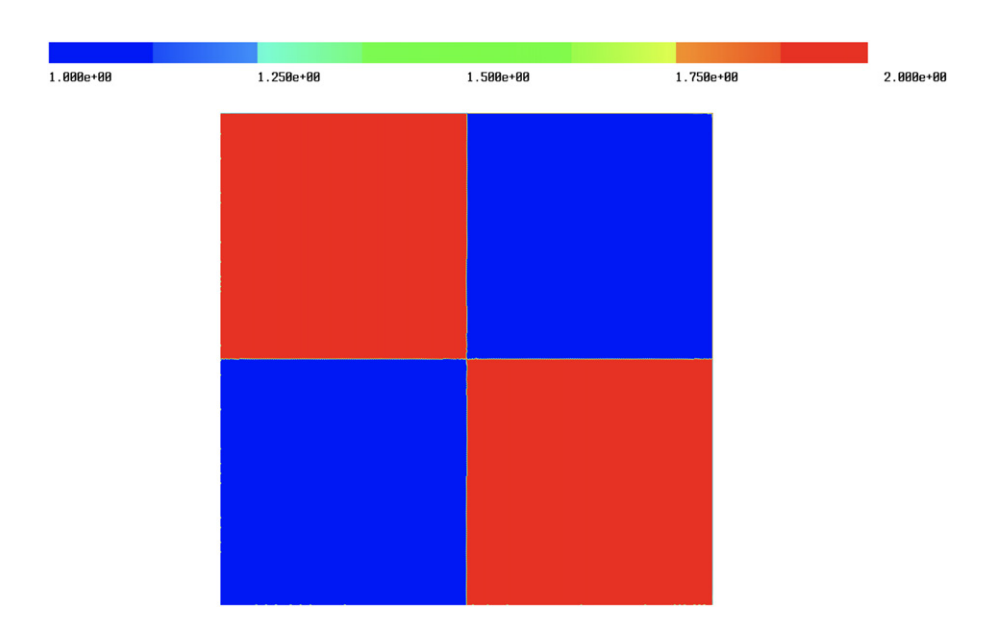


Figure 14. n(y) defined as in (40) plotted on cell $Y = [0, 1] \times [0, 1]$.

n(x), as shown in figure 12. We also vary the radius at which we read our data. Note that as our data approach ∂D , the n is better resolved. However, the approximations of n produced from reading a bit further away ∂D , namely at r=1.5 and r=1.99, are still reasonable. In figure 13 we show the same simulation results for a square scatterer, $D=(-0.5,-0.5)\times(0.5,0.5)$. For the case of the square scatterer, we read the error in the scattered field on the circle centered at the origin of radius 1.

6.3.3. Checkerboard. For the next example, we choose a piecewise-constant periodic n varying in two dimensions given by

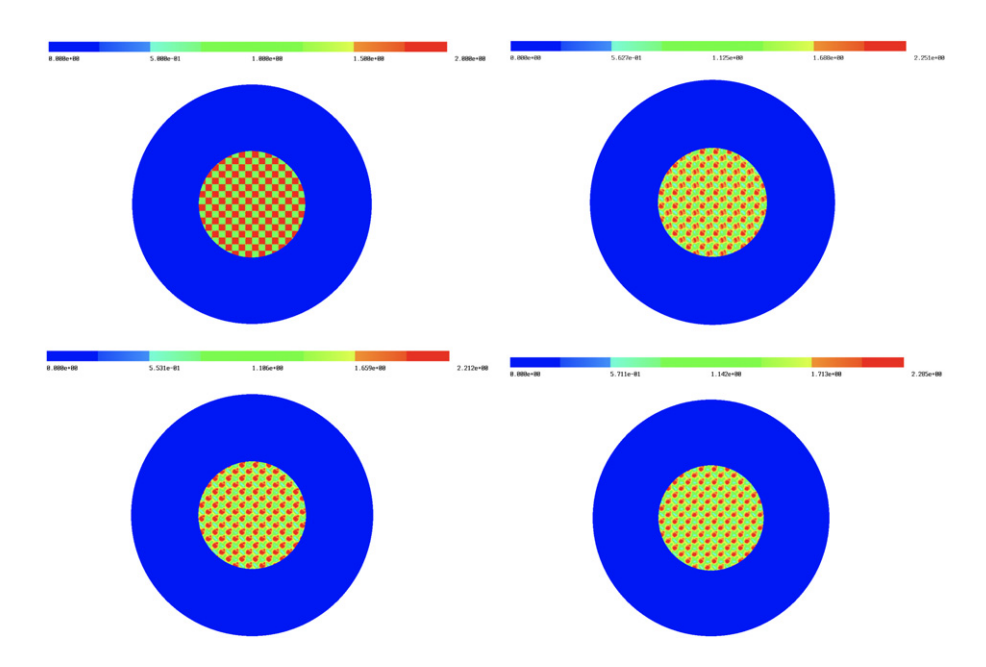


Figure 15. Results of numerical inversion with $n(x/\epsilon)$ given by (40) and recovered n plotted on the circular scatterer D of radius 1, $\epsilon = 1/4$. Top left: true solution n, top right: recovered n reading data in the scattered field on the circles r = 1.1, bottom left: recovered n reading the data in the scattered field on the circle r = 1.5, bottom right: recovered n reading the data in the scattered field on the circle r = 1.99.

$$n(y) = \begin{cases} 1 & y_1 \in [0, 0.5), y_2 \in [0, 0.5) \\ 2 & y_1 \in [0, 0.5), y_2 \in [0.5, 1) \\ 2 & y_1 \in [0.5, 1), y_2 \in [0, 0.5) \\ 1 & y_1 \in [0.5, 1), y_2 \in [0.5, 1) \end{cases}$$

$$(40)$$

as shown in figure 14. Once again, we assume we know ϵ , the location of the scatterer D, and that the interior of the scatterer has a periodic structure by modeling n using two-dimensional, smoothly varying periodic elements. Numerical results in figure 15 show the accuracy of the first order approximation in recovery of qualitative properties of n(x) when D is a circle. Once again, we show results for varying radii at which we read the data. Results in figure 16 show our recovery for the checkerboard when D is a square.

Remark 6.1. The above reconstruction approach recovers the small highly oscillating part of the refractive index as perturbation of the effective homogenized medium, meaning that \overline{n} and the support D are known. These are not restrictive assumptions since from the same type of data we use, one can first determine the ∂D by means of any of the linear or factorization methods [13] which can reconstruct the support without any knowledge of the refractive index. Furthermore, if such data is collected for a range of frequencies, it is possible to determine the lowest transmission eigenvalue corresponding to the inhomogeneity [13], which for the current case, is sufficient to estimate the constant \overline{n} , as discussed e.g. in [11]. The inversion method here also assumes periodicity and the knowledge of the period ϵ , but no other *apriori*

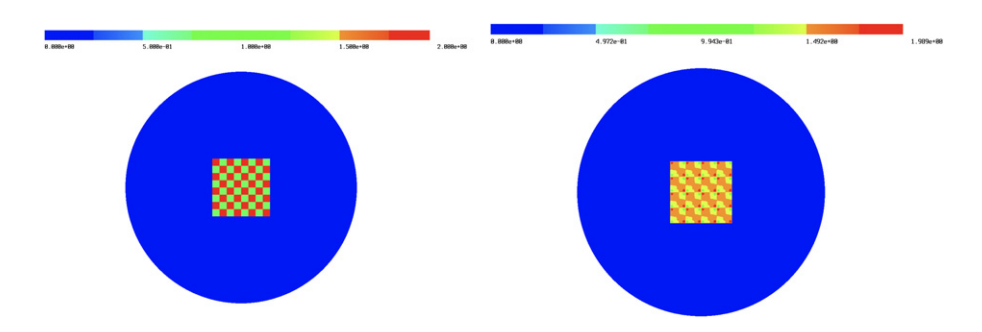


Figure 16. Results of numerical inversion with $n(x/\epsilon)$ given by (40) (left) and recovered n (right) plotted on the square scatterer $D=(-0.5,-0.5)\times(0.5,0.5)$, $\epsilon=1/4$. Data is read at a radius of r=1.

information about the medium. We believe that a detailed asymptotic analysis of the transmission eigenvalue problem with explicit first correction term will allow us to estimate the period from the measured first transmission eigenvalue, and we plan to pursue this in a forthcoming study.

Acknowledgments

The research of F. Cakoni is partially supported by the AFOSR Grant FA9550-20-1-0024 and NSF Grant DMS-1813492. F. Cakoni also acknowledges support from the NSF HDR TRIPODS award CCF-1934924. The work of SM is supported in part by NSF Grant DMS1715425.

ORCID iDs

Fioralba Cakoni https://orcid.org/0000-0002-4648-8780 Shari Moskow https://orcid.org/0000-0002-8240-7247

References

- [1] Allaire G 1992 Homogenization and two-scale convergence SIAM J. Math. Anal. 23 1482-518
- [2] Allaire G 2002 Shape Optimization by the Homogenization Method (New York, NY: Springer)
- [3] Allaire G and Amar M 1999 Boundary layer tails in periodic homogenization ESAIM: Control Optim. Calculus Var. 4 209-43
- [4] Allaire G, Briane M and Vanninathan M 2016 A comparison between two-scale asymptotic expansions and block wave expansions for the homogenization of periodic structures SeMA J. 73 237-59
- [5] Andrianov I V, Bolshakov V I, Danishevskyy V and Weichert D 2008 Higher order asymptotic homogenization and wave propagation in periodic composite materials *Proc. R. Soc.* A 464 1181–201
- [6] Avellaneda M and Lin F-H 1987 Homogenization of elliptic problems with L^p boundary data Appl. Math. Optim. 15 93–107
- [7] Bensoussan A, Lions J L and Papanicolaou G 1978 Asymptotic Analysis for Periodic Structures (Providence, RI: AMS Chelsea Publishing)

- [8] Bouchitté G, Bourel C and Felbacq D 2009 Homogenization of the 3D Maxwell system near resonances and artificial magnetism C. R. Math. Acad. Sci., Paris 347 571–6
- [9] Cakoni F and Colton D 2014 Qualitative Approach to Inverse Scattering Theory (New York, NY: Springer)
- [10] Cakoni F, Guzina B B, Moskow S and Pangburn T 2019 Scattering by a bounded highly oscillating periodic medium and the effect of boundary correctors SIAM J. Appl. Math. 79 1448–74
- [11] Cakoni F, Haddar H and Harris I 2015 Homogenization of the transmission eigenvalue problem for periodic media and application to the inverse problem *Inverse Problems Imaging* **9** 1025–49
- [12] Cakoni F, Guzina B B and Moskow S 2016 On the homogenization of a scalar scattering problem for highly oscillating anisotropic media SIAM J. Math. Anal. 48 2532–60
- [13] Cakoni F, Colton D and Haddar H 2016 *Inverse Scattering Theory and Transmission Eigenvalues* (CBMS Series) (Philadelphia, PA: SIAM Publications) p 88
- [14] Craster R V, Joseph L M and Kaplunov J 2014 Long-wave asymptotic theories: the connection between functionally graded waveguides and periodic media Wave Motion 52 581–8
- [15] Craster R V, Kaplunov J and Pichugin A V 2010 High-frequency homogenization for periodic media Proc. R. Soc. A 466 2341–62
- [16] Craster R V, Kaplunov J, Nolde E and Guenneau S 2012 Bloch dispersion and high frequency homogenization for separable doubly-periodic structures Wave Motion 49 333–46
- [17] Christensen J and Javier Garcia de Abajo F 2012 Anisotropic metamaterials for full control of acoustic waves Phys. Rev. Lett. 108 124301
- [18] Colombi A, Roux P, Guenneau S, Gueguen P and Craster R V 2016 Forests as a natural seismic metamaterial: Rayleigh wave bandgaps induced by local resonances Sci. Rep. 6 19238
- [19] Gérard-Varet D and Masmoudi N 2012 Homogenization and boundary layers *Acta Math.* **209**
- [20] Gérard-Varet D and Masmoudi N 2012 Homogenization in polygonal domains J. Eur. Math. Soc. 11 1477–503
- [21] Griso G 2004 Error estimates and unfolding for periodic homogenization *Asymptotic Anal.* **40** 269–86
- [22] Guzina B B, Meng S and Oudghiri-Idrissi O 2019 A rational framework for dynamic homogenization at finite wavelengths and frequencies *Proc. R. Soc.* A 475 20180547
- [23] Kafesaki M and Economou E N 2014 Multiple-scattering theory for three-dimensional periodic acoustic composites Phys. Rev. B 60 11993
- [24] Kenig C E, Lin F and Shen Z 2013 Estimates of eigenvalues and eigenfunctions in periodic homogenization J. Eur. Math. Soc. 15 1901–25
- [25] Kenig C E, Lin F and Shen Z 2012 Convergence rates in L^2 for elliptic homogenization problems *Arch. Ration. Mech. Anal.* **203** 1009–36
- [26] Kenig C E, Lin F and Shen Z 2013 Homogenization of elliptic systems with Neumann boundary conditions J. Am. Math. Soc. 26 901–37
- [27] Lions J L 1981 Some Methods for the Mathematical Analysis of Systems (Beijing: Science Press)
- [28] Marchenko V A and Khruslov E Y 2006 *Homogenization of Partial Differential Equations* (Basel: Birkhaäuser)
- [29] Maz'ya V G, Movchan A B and Nieves M J 2013 *Green's Kernels and Meso-Scale Approximations in Perforated Domains* (Lecture Notes in Mathematics vol 2077) (Berlin: Springer)
- [30] Maz'ya V G, Nazarov S and Plamenevskij B 2000 Asymptotic Theory of Elliptic Boundary Value Problems in Singularly Perturbed Domains I (Basel: Birkhaäuser)
- [31] Maz'ya V G, Nazarov S and Plamenevskij B 2000 Asymptotic Theory of Elliptic Boundary Value Problems in Singularly Perturbed Domains II (Basel: Birkhaäuser)
- [32] Meng S and Guzina B B 2018 On the dynamic homogenization of periodic media: Willis approach versus two-scale paradigm *Proc. R. Soc.* A 474 20170638
- [33] Moskow S and Vogelius M 1997 First-order corrections to the homogenized eigenvalues of periodic composite material. A convergence proof *Proc. R. Soc. Edinburgh A* 127 1263–99
- [34] Moskow S and Vogelius M 1997 First-order corrections to the homogenized eigenvalues of periodic composite material. The case of Neumann boundary conditions
- [35] Neacsu C C, Berweger S, Olmon R L, Saraf L V, Ropers C and Raschke M B 2010 Near-field localization in plasmonic superfocusing: a nanoemitter on a tip *Nano Lett.* 10 592–6
- [36] J. Schöberl Netgen/NGSolve finite element library https://ngsolve.org (accessed in 2019)
- [37] Onofrei D and Vernescu B 2007 Error estimates for periodic homogenization with non-smooth coefficients *Asymptotic Anal.* **54** 103–23

- [38] Onofrei D and Vernescu B 2012 Asymptotic analysis of second-order boundary layer correctors Appl. Anal. 91
- [39] Oudich M and Li Y 2017 Tunable sub-wavelength acoustic energy harvesting with a metamaterial plate *J. Phys. D: Appl. Phys.* **50** 315104
- [40] Santosa F and Symes W 1991 A dispersive effective medium for wave propagation in periodic composites SIAM J. Appl. Math. 51 984–1005
- [41] Santosa F and Vogelius M 1993 First-order corrections to the homogenized eigenvalues of periodic composite medium SIAM J. Appl. Math. 53 1636–68
- [42] Sarkis M and Versieux H 2008 Convergence analysis for the numerical boundary corrector for elliptic equations with rapidly oscillating coefficients SIAM J. Numer. Anal. 46 545–76
- [43] Vinoles V 2016 Problémes d'interface en presence de métamatériaux: Modélisation, analyse et simulations *Thése de Doctoratés Mathématiques* Université Paris-Saclay
- [44] Wautier A and Guzina B B 2015 On the second-order homogenization of wave motion in periodic media and the sound of a chessboard J. Mech. Phys. Solids 78 382–414